

On the Design of Control Invariant Regions for Feedback Linearized Car-Like Vehicles

Cristian Tiriolo and Walter Lucia *Member, IEEE*

Abstract—This paper proposes a novel procedure to design a control invariant region for feedback-linearized car-like vehicles subject to linear and steering velocity constraints. To this end, first, it is formally proved that the state-dependent input constraints acting on the feedback-linearized car model admit a worst-case circular inner approximation. Then, it is shown that such a characterization can be used to analytically design a tracking controller with an associated invariant region capable of ensuring constraints fulfillment. Finally, simulation results show the effectiveness of the proposed solution and its potential to enable the design, via control invariance, of a new class of constrained and model predictive solutions for input-constrained feedback-linearized car-like vehicles.

Index Terms—Autonomous vehicles; Constrained control; Feedback linearization

I. INTRODUCTION

In the autonomous driving field, trajectory tracking is a critical task necessary to guarantee the full autonomy of the vehicle [1]. If car-like vehicles are considered, one of the related difficulties to consider is the nonholonomic nature of their kinematics [2]. In particular, such vehicles do not satisfy the Brockett conditions and it is not possible to design a smooth stabilizing static feedback control law [3].

Among existing strategies, Model Predictive Control (MPC) has been successfully applied to solve reference tracking problems in the presence of constraints [4]. MPC techniques can be classified into two classes: nonlinear MPC formulations, which exploit a nonlinear model of the car to predict its future behaviour, and linear MPC schemes that leverage linearized model descriptions. Although, in principle, nonlinear MPC formulations are preferable, given their accuracy in the predictions, the resulting optimization is highly nonlinear and nonconvex. Consequently, the resulting strategies might not be real-time affordable if the available computational power is limited and the used solvers suffer from unavoidable local minima that might be far from the global optimum [5]. On the other hand, linear MPC formulations do not suffer from the above drawbacks. However, linearized descriptions have been found to be suboptimal and less performing with respect to the nonlinear counterpart due to the approximations introduced by the linearization process [6].

This work was supported by the Natural Sciences and Engineering Research Council of Canada (NSERC).

Cristian Tiriolo and Walter Lucia are with the Concordia Institute for Information Systems Engineering (CIISE), Concordia University, Montreal, QC, H3G 1M8, CANADA, cristian.tiriolo@concordia.ca, walter.lucia@concordia.ca

In order to preserve the accuracy of nonlinear MPC formulations and obtain affordable optimization problems, the joint use of feedback linearization techniques and MPC has been investigated. Unfortunately, such an approach leads to quadratic programming problems only for unconstrained models [7]. It has been shown that, via feedback linearization, time-invariant input constraints recast into nonlinear, time-dependent, and non-convex constraints [7]. This aspect makes it hard to characterize constrained control laws and the associated invariant regions for car-like vehicles via feedback linearization. Consequently, also any MPC tracking controller consisting of a finite prediction horizon and terminal invariant region (capable of ensuring stability and recursive feasibility) [8], [9] cannot be used on the feedback linearized car-like model.

A. Paper's contribution

In general, the literature lacks solutions where control invariance theory [10] is used to ensure safety and reference tracking for constrained feedback linearized car-like vehicles, as instead exploited for approximated linearized descriptions in, e.g., [11]–[13]. This paper addresses this gap and proposes a procedure to analytically design a tracking controller and associated control invariant region for an input-output feedback linearized car-like model subject to linear and angular velocities constraints. First, we resort to geometrical considerations to formally characterize the time-varying constraints set arising via feedback linearization. Then, we analytically characterize its worst-case and time-invariant circular approximation and analytically design a stabilizing tracking controller and associated safe invariant region. In a nutshell, the proposed characterization of the worst-case input constraint set and control invariant regions defines a new control approach for car-like vehicles that paves the way to the future design of novel reference tracking control schemes (e.g., constrained/robust controllers) with safety guarantees for constrained car-like vehicles. For example, the proposed controller can be used as the terminal controller/region of novel model predictive control strategies with safety guarantees [8], [9].

II. PRELIMINARIES AND PROBLEM FORMULATION

Given a matrix M and a vector v , $M[i, :]$ denotes the i -th row of M , $M[i, j]$ the (i, j) entry of M , and $v[i]$ the i -th element of v . A function $f(t)$ is said of class C^2 if $f(t)$ admits two continuous derivatives in its domain.

Definition 1: Given an autonomous discrete-time linear system $x(k+1) = Ax(k)$ subject to the state constraint $x(k) \in \mathcal{X}$. A set $\Sigma \subseteq \mathcal{X}$ is said positively invariant if $\forall x(0) \in \Sigma \implies x(k) \in \Sigma, \forall k > 0$ [14].

Definition 2: A tracking controller is said to have a control invariant region if the tracking error can be confined in an a priori known bounded region.

A. Car-like vehicle modeling

A car-like vehicle is a nonholonomic wheeled vehicle consisting of two rear drive wheels and two front wheels. By assuming rear driving wheels, its kinematic can be described in the continuous-time domain as in [3]:

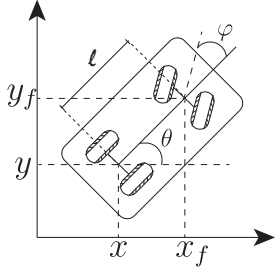


Fig. 1. Car-like vehicle

$$\dot{q}_c(t) = \begin{bmatrix} \dot{x}(t) \\ \dot{y}(t) \\ \dot{\theta}(t) \\ \dot{\varphi}(t) \end{bmatrix} = \begin{bmatrix} \cos \theta(t) \\ \sin \theta(t) \\ \frac{1}{l} \tan(\varphi(t)) \\ 0 \end{bmatrix} v(t) + \begin{bmatrix} 0 \\ 0 \\ 0 \\ 1 \end{bmatrix} \omega(t) \quad (1)$$

where $q_c = [x, y, \theta, \varphi]^T$ is the car's state vector. By referring to Fig. 1, x and y are the Cartesian coordinates of the rear axis' midpoint, θ is the orientation of the vehicle with respect to the x -axis, $\varphi \in (-\pi/2, \pi/2)$ is the steering angle, and $u = [v, \omega]^T$ are the control inputs, i.e., the linear velocity of the vehicle and the steering angular velocity respectively. Moreover, l is a geometrical parameter representing the distance between the front and rear wheels, and

$$x_f = x + l \cos \theta \quad y_f = y + l \sin \theta$$

are the Cartesian coordinates of the front axis' midpoint. The car's control inputs are subject to the following symmetrical constraints

$$u(t) \in \mathcal{U}_{car} := \{u \in \mathbb{R}^2 : Tu \leq g\} \quad (2)$$

where

$$T = \begin{bmatrix} -1 & 0 \\ 0 & -1 \\ 1 & 0 \\ 0 & 1 \end{bmatrix}, \quad g = \begin{bmatrix} \bar{v} \\ \bar{\omega} \\ \bar{v} \\ \bar{\omega} \end{bmatrix}$$

and $\bar{v}, \bar{\omega} > 0$ are given upper bounds.

B. Input-Output Feedback Linearization

As outlined in [3], an input-output feedback linearized model of (1) can be obtained by defining two new auxiliary outputs

$$z = \begin{bmatrix} z_1 \\ z_2 \end{bmatrix} = \begin{bmatrix} x + l \cos(\theta) + \Delta \cos(\theta + \varphi) \\ y + l \sin(\theta) + \Delta \sin(\theta + \varphi) \end{bmatrix} \quad (3)$$

and by applying to the nonlinear car model (1) the following state-dependent input transformation:

$$w = M(\theta, \varphi)u, \quad M(\theta, \varphi) = \begin{bmatrix} \cos \theta - \tan \varphi (\sin \theta + \frac{\Delta}{l} \sin(\psi)) & -\Delta \sin(\psi) \\ \sin \theta + \tan \varphi (\cos \theta + \frac{\Delta}{l} \cos(\psi)) & \Delta \cos(\psi) \end{bmatrix} \quad (4)$$

where $\psi = \theta + \varphi$, the following feedback linearized model of (1) is obtained:

$$\begin{bmatrix} \dot{z}_1 \\ \dot{z}_2 \end{bmatrix} = \begin{bmatrix} 1 & 0 \\ 0 & 1 \end{bmatrix} \begin{bmatrix} w_1 \\ w_2 \end{bmatrix} \quad (5a)$$

$$\begin{bmatrix} \dot{\theta} \\ \dot{\varphi} \end{bmatrix} = O(\theta, \varphi) \begin{bmatrix} w_1 \\ w_2 \end{bmatrix} \quad (5b)$$

where

$$O(\theta, \varphi) = \begin{bmatrix} \frac{\sin \varphi \cos(\psi)}{l} & \frac{\sin \varphi \sin(\psi)}{l} \\ -\frac{\cos(\psi) \sin \varphi}{l} - \frac{\sin(\psi)}{\Delta} & -\frac{\sin(\psi) \sin \varphi}{l} + \frac{\cos(\psi)}{\Delta} \end{bmatrix}$$

Note that (5b) defines nonlinear internal dynamics decoupled from (5a). Moreover, by considering the input transformation (4), the set of feasible inputs $w = [w_1, w_2]^T$ for (5) is

$$w \in \mathcal{U}(\theta, \varphi) = \{w \in \mathbb{R}^2 : L(\theta, \varphi)w \leq g\}, \quad L = TM^{-1} \quad (6)$$

In what follows, by referring to the representation of (6) in Fig. 2 (the blue polyhedral region), we denote with $L_i, i = 1, \dots, 4$ the line defined by $L[i, :](\theta, \varphi)w = g[i]$, and with l_i the size of the corresponding edge of $\mathcal{U}(\theta, \varphi)$. Moreover, $m(L_i)$ defines the angular coefficient of the line L_i .

C. Problem's statement

Problem 1: Design a tracking controller with associated control invariant region for the tracking error of the feedback linearized car-like model (5) subject to the time-varying input constraint (6).

III. PROPOSED SOLUTION

In this section, the considered problem is split into two parts. First, the input constraint set (6) is characterized and its worst-case inner approximation formally derived. Then, a procedure to analytically design a constrained tracking controller with associated control invariant region is presented.

A. Input constraints characterization

The constraint set $\mathcal{U}(\theta, \varphi)$ defines in \mathbb{R}^2 a two-dimensional state-dependent and time-varying polyhedron (see Fig. 2). The geometry and properties of $\mathcal{U}(\theta, \varphi)$ are characterized in Proposition 1. Furthermore, Proposition 2 analytically derives a worst-case and time-invariant inner approximation of $\mathcal{U}(\theta, \varphi)$, namely $\hat{\mathcal{U}}$ (the red circle in Fig. 2).

Proposition 1: The time-varying input constraint set (6) is a parallelogram shaped set centered in 0_2 whose vertices are

$$V_1 = \begin{bmatrix} \frac{\Delta s_1 l \bar{\omega} + \Delta \sin(\theta) l \bar{\omega} + \Delta \bar{v} \cos(\theta) - \Delta \bar{v} c_1 - 2c_2 l \bar{v}}{2l \cos(\varphi)} \\ \frac{-\bar{\omega} \Delta l \cos(\theta) - \bar{\omega} \Delta l c_1 - \Delta s_1 \bar{v} + \Delta \sin(\theta) \bar{v} - 2s_2 l \bar{v}}{2l \cos(\varphi)} \end{bmatrix} \quad (7a)$$

$$V_2 = \begin{bmatrix} \frac{-\Delta s_1 l \bar{\omega} - \Delta \sin(\theta) l \bar{\omega} + \Delta \bar{v} \cos(\theta) - \Delta \bar{v} c_1 - 2c_2 l \bar{v}}{2l \cos(\varphi)} \\ \frac{\bar{\omega} \Delta l \cos(\theta) + \bar{\omega} \Delta l c_1 - \Delta s_1 \bar{v} + \Delta \sin(\theta) \bar{v} - 2s_2 l \bar{v}}{2l \cos(\varphi)} \end{bmatrix} \quad (7b)$$

$$V_1 = -V_3, \quad V_2 = -V_4 \quad (7c)$$

and that rotates according to $\theta(t)$ and $\varphi(t)$.

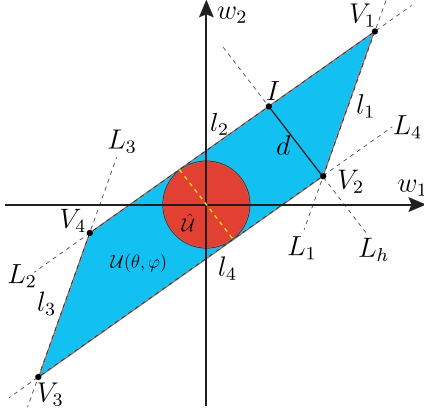


Fig. 2. Time-varying input constraint set and its worst-case approximation

Proof: The shaping matrix $L(\theta, \varphi)$ of the polyhedral set (6) can be explicitly re-written as:

$$L(\theta, \varphi) = \begin{bmatrix} \frac{-\cos(\theta)+c_1}{2} & \frac{-\sin(\theta)+s_1}{2} \\ \frac{\Delta s_1 - \Delta \sin(\theta) + 2ls_2}{2\Delta l} & \frac{-\Delta c_1 + \Delta \cos(\theta) - 2lc_2}{2\Delta l} \\ \frac{\cos(\theta)+c_1}{2} & \frac{\sin(\theta)+s_1}{2} \\ \frac{-\Delta s_1 - \Delta \sin(\theta) + 2ls_2}{2\Delta l} & \frac{-\Delta c_1 + \Delta \cos(\theta) - 2lc_2}{2\Delta l} \end{bmatrix}$$

where

$$\begin{aligned} c_1 &= \cos(\theta + 2\varphi), & c_2 &= \cos(\theta + \varphi) \\ s_1 &= \sin(\theta + 2\varphi), & s_2 &= \sin(\theta + \varphi) \end{aligned}$$

By intersecting the four hyperplanes characterizing the polyhedron, the vertices V_i , $i = 1 \dots 4$ in (7) are obtained (see Fig. 2). Consequently, for symmetry, $\mathcal{U}(\theta, \varphi)$ is centred in 0 , $\forall \theta \in \mathbb{R}, \forall \varphi \in (-\pi/2, \pi/2)$. By resorting to simple geometric arguments, the values of l_i , $i = 1, 2, 3, 4$ are

$$\begin{aligned} l_1 &= l_3 = 2\sqrt{\Delta^2 \bar{\omega}^2} \\ l_2 &= l_4 = 2\sqrt{\frac{v_1^2(-\Delta^2 \cos(2\varphi) + \Delta^2 + 2l^2)}{l^2(\cos(2\varphi) + 1)}} \end{aligned} \quad (8)$$

and $m(L_1) = m(L_3)$, $m(L_2) = m(L_4)$, i.e., L_1 and L_3 , and L_2 and L_4 are mutually parallel (see Fig. 2). Moreover, l_1 and l_3 are independent of $\theta(t)$ and $\varphi(t)$ and their values depend on the parameters Δ and $\bar{\omega}$. On the other hand, l_2 and l_4 are time-varying and their value is a function of $\varphi(t)$. Furthermore, l_2 and l_4 are minimal for $\varphi = 0$ and monotonically increase with the module of φ until $\pi/2$ (from the left) or $-\pi/2$ (from the right) is approached. Consequently, by collecting all the above, it results that $\mathcal{U}(\theta, \varphi)$ is a time-varying parallelogram-shaped region centred in 0_2 that rotates around the origin according to θ and φ . ■

B. Worst-Case Inner Approximation

The following proposition describes the inner and time-invariant worst-case approximation $\hat{\mathcal{U}} \subset \mathcal{U}(\theta, \varphi)$ complying with the cars' input constraint (2) $\forall \theta \in \mathbb{R}, \varphi \in (-\pi/2, \pi/2)$.

Proposition 2: If $l_1 < l_2$, the worst-case constraint set inscribed in $\mathcal{U}(\theta(t), \varphi(t))$, $\forall \theta(t) \in \mathbb{R}, \forall \varphi(t) \in (-\pi/2, \pi/2)$ is a circular region $\hat{\mathcal{U}}$ of radius $\hat{r} > 0$ centered in 0_2 , i.e.,

$$\hat{\mathcal{U}} = \{w \in \mathbb{R}^2 \mid w^T \frac{1}{\hat{r}^2} I_{2 \times 2} w \leq 1\}, \hat{r} = \Delta l \bar{\omega} \sqrt{\frac{1}{\Delta^2 + l^2}} \quad (9)$$

Proof: First, for any fixed value of φ , the polyhedral set $\mathcal{U}(\theta(t), \varphi(t))$ rigidly rotates in the plane around 0_2 describing a circle centered at the origin (see Fig. 2). Moreover, since only l_2 and l_4 are a function of φ , the radius of the circle changes with $\varphi \in (-\pi/2, \pi/2)$. By observing the geometry of $\mathcal{U}(\theta, \varphi)$ in Fig. 2, if $l_1 < l_2$, every segment orthogonal to the edges l_2 and l_4 corresponds to the height of $\mathcal{U}(\theta(t), \varphi(t))$, namely $d > 0$, and to the diameter of the inner circular region. On the other hand, d is equal to the length of the segment $\overline{IV_2}$, where I is the intersection point between L_2 and the line, namely L_h , passing by V_2 and orthogonal to L_2 . By noting that the equation describing L_2 can be obtained considering the second row of $L(\theta, \varphi)$ and g , we have

$$\begin{aligned} L_2: & \alpha(\theta, \varphi)w_1 + \beta(\theta, \varphi)w_2 = \gamma \\ \alpha(\theta, \varphi) &= L[2, 1], \quad \beta(\theta, \varphi) = L[2, 2], \quad \gamma = g[2] \end{aligned} \quad (10)$$

which can be re-written as:

$$\begin{aligned} L_2: & w_2 = m(\theta, \varphi)w_1 + h(\theta, \varphi) \\ m(\theta, \varphi) &= -\frac{\alpha(\theta, \varphi)}{\beta(\theta, \varphi)}, \quad h(\theta, \varphi) = \frac{\gamma}{\beta(\theta, \varphi)} \end{aligned} \quad (11)$$

Consequently, the equation describing L_h is

$$L_h: w_2 - V_2[2] = -\frac{1}{m(\theta, \varphi)}(w_1 - V_2[1]) \quad (12)$$

Given L_2 and L_h , the intersection point I is given by the following linear system:

$$\begin{bmatrix} -m(\theta, \varphi) & 1 \\ \frac{1}{m(\theta, \varphi)} & 1 \end{bmatrix} I = \begin{bmatrix} h(\theta, \varphi) \\ \frac{V_2[1]}{m} + V_2[2] \end{bmatrix} \quad (13)$$

which admits a single solution

$$I = \begin{bmatrix} -m(\theta, \varphi) & 1 \\ \frac{1}{m(\theta, \varphi)} & 1 \end{bmatrix}^{-1} \begin{bmatrix} h(\theta, \varphi) \\ \frac{V_2[1]}{m(\theta, \varphi)} + V_2[2] \end{bmatrix} \quad (14)$$

Then, the radius $r(\varphi)$ of the circle inscribed in $\mathcal{U}(\theta, \varphi)$ can be computed as:

$$\begin{aligned} r(\varphi) &= \frac{1}{2}d = \frac{1}{2}\sqrt{(I - V_2)^T(I - V_2)} = \\ &= \Delta l \bar{\omega} \sqrt{\frac{1}{\Delta^2 - \Delta^2 \cos^2(\varphi) + l^2}} \end{aligned} \quad (15)$$

Hence, the value of $r(\varphi)$ decreases as φ approaches $\pi/2$ from the left or $-\pi/2$ from the right. In conclusion, the radius \hat{r} of the worst case (smallest) circular region can be obtained by $r(\varphi)$ for φ approaching $\pm\pi/2$, i.e.,

$$\hat{r} = \lim_{|\varphi| \rightarrow \frac{\pi}{2}} r(\varphi) = \Delta l \bar{\omega} \sqrt{\frac{1}{\Delta^2 + l^2}} \quad (16)$$

and $\hat{\mathcal{U}}$ can be written as in (9), concluding the proof. ■

C. Linearized tracking-error model

Consider an arbitrary reference trajectory described in terms of cartesian positions $x_r(t)$, $y_r(t)$, velocities $\dot{x}_r(t)$, $\dot{y}_r(t)$, accelerations $\ddot{x}_r(t)$, $\ddot{y}_r(t)$, and jerks $\dddot{x}_r(t)$, $\dddot{y}_r(t)$. Then, by considering (1), the reference values associated to the considered trajectory for the linear velocity $v_r(t)$, steering

angular velocity $\omega_r(t)$, orientation $\theta_r(t)$, and steering angle $\varphi_r(t)$ are [3]:

$$\begin{aligned} u_r(t) &= \left[lv_r \frac{\sqrt{\dot{x}_r(t)^2 + \dot{y}_r(t)^2}}{v_r^6 + l^2(\dot{y}_r \dot{x}_r - \dot{x}_r \dot{y}_r)^2} \right] \\ \theta_r(t) &= \text{ATAN}_2 \left(\frac{\dot{y}_r(t)}{v_r(t)}, \frac{\dot{x}_r(t)}{v_r(t)} \right) \\ \varphi_r(t) &= \arctan \left(\frac{l(\dot{y}_r(t)\dot{x}_r(t) - \dot{x}_r(t)\dot{y}_r(t))}{v_r(t)^3} \right) \end{aligned} \quad (17)$$

Assumption 1: The reference trajectory $q_r(t) = [x_r(t), y_r(t), \theta_r(t), \varphi_r(t)]^T$ for (1) is uniformly bounded and smooth, i.e., $\exists \Gamma > 0 : \|q_r(t)\| < \Gamma, \forall t \geq 0, q_r(t) \in \mathcal{C}^2$. \square

Definition 3: Consider the car model (1) and a reference trajectory $q_r(t)$ complying with Assumption 1. By considering the tracking error with respect to the reference trajectory, namely $\tilde{q}(t) = q_c(t) - q_r(t)$, stable full-state tracking is achieved if for any $\varepsilon > 0$, there exists $\delta(\varepsilon) > 0, t_0 \geq 0$ such that $\|\tilde{q}(t_0)\| < \delta(\varepsilon) \implies \|\tilde{q}(t)\| < \varepsilon, \forall t \geq t_0$ [15]. \square

By resorting to the transformation (3), the Cartesian reference signal $[x_r, y_r]^T$ translated into the feedback linearized car model (5a), namely z_r , is

$$z_r = \begin{bmatrix} x_r + l \cos(\theta_r) + \Delta \cos(\theta_r + \varphi_r) \\ y_r + l \sin(\theta_r) + \Delta \sin(\theta_r + \varphi_r) \end{bmatrix}$$

Consequently, by defining the tracking error for (5a) as $\tilde{z}(t) = z(t) - z_r(t)$, the error dynamics are:

$$\dot{\tilde{z}}(t) = \tilde{w}(t), \quad (18a)$$

$$\tilde{w}(t) = w(t) - w_r(t), \quad w_r(t) = M(\theta_r(t), \varphi_r(t))u_r(t) \quad (18b)$$

Lemma 1: Consider a reference trajectory $q_r(t)$ complying with Assumption 1 with $v_r(t)$ and $\omega_r(t)$ satisfying (17) and such that

$$0 < v_r(t) \leq V, V > 0 \quad \text{and} \quad \forall |\varphi_r(t)| \leq \frac{\pi}{2}, \quad \forall t \quad (19)$$

Then, the tracking-error zero dynamics with respect to q_r are asymptotically stable [15, Theorems 1-3]. Consequently, if a generic control law $\tilde{w}(t)$ stabilizes (18a), then stable full-state tracking is achieved [15]. \square

D. Tracking controller and associated control invariant set

In this subsection, the worst-case input constraint set \hat{U} is used to design a constrained tracking controller with associated control invariant region. By considering a sufficiently small sampling time interval $T_s > 0$ and by resorting to a ZOH discretization method, the discretized model of (18) is

$$\tilde{z}(k+1) = A\tilde{z}(k) + Bw(k) - Bw_r(k), \quad (20a)$$

$$w(k) \in \mathcal{U}(\theta(k), \varphi(k)) \quad (20b)$$

where $A = I_{2 \times 2}$, $B = T_s I_{2 \times 2}$.

Remark 1: For the considered car-like model (1) and ZOH discretization method, it is straightforward to prove that discretization and feedback linearization commute. \square

Since the reference signal is bounded (see Assumption 1), then $w_r(k)$ in (20a) is bounded and the term $-Bw_r(k)$ can be

considered as a disturbance. As a consequence, a stabilizing controller can be designed starting from the disturbance-free model

$$\tilde{z}(k+1) = A\tilde{z}(k) + Bw(k) \quad (21)$$

By considering (21), a Linear-Quadratic (LQ) state-feedback control law

$$w(k) = -K\tilde{z}(k) \quad (22)$$

can be designed such that

$$\tilde{z}(k+1) = (A - BK)\tilde{z}(k) \quad (23)$$

is asymptotically stable. The following proposition shows that given the structure of (21), the LQ design problem admits, for a proper choice of the cost, an analytical solution. Such a point is instrumental in showing (see Theorem 1) the existence of a control invariant region associated with the LQ controller.

Proposition 3: Consider the following discrete-time infinite horizon LQ cost

$$J(w(k)) = \sum_{k=0}^{\infty} \tilde{z}(k)^T Q \tilde{z}(k) + w(k)^T R w(k), \quad Q \geq 0, R > 0 \quad (24)$$

for the linear system (20) under the control law (22). If the LQ weighting matrices are $Q = qI_{2 \times 2}$ and $R = \rho I_{2 \times 2}$ with $q, \rho > 0$, the control gain K minimizing $J(w(k))$ is

$$K = \kappa I, \quad \kappa = \frac{qT_s^2 + \sqrt{qT_s^2(T_s^2 q + 4\rho)}}{(qT_s^2 + \sqrt{qT_s^2(T_s^2 q + 4\rho)} + 2\rho)T_s} \quad (25)$$

Proof: Since for (20) the pair (A, B) is stabilizable, for any $Q = Q_z^T Q_z \geq 0$ and $R > 0$ such that (A, Q_z) is detectable, the gain K that ensure a finite and minimal value of $J(w(k))$ is

$$K = (B^T P B + R)^{-1} B^T P A \quad (26)$$

where $P = P^T > 0$ is the only symmetric and positive-definite solution to the following Discrete-time Algebraic Riccati Equation (DARE) [16]:

$$A^T P A - P - A^T P B (B^T P B + R)^{-1} B^T P A + Q = 0 \quad (27)$$

Since for (20), $A = I_{2 \times 2}$ and $B = T_s I_{2 \times 2}$, if $Q = qI_{2 \times 2}$ and $R = \rho I_{2 \times 2}$, the equation (27) can be analytically solved, obtaining

$$P = pI_{2 \times 2}, \quad p = \frac{qT_s^2 + \sqrt{T_s^4 q^2 + 4T_s^2 q\rho}}{2T_s^2}$$

Finally, by substituting the obtained P into (26), the gain K in (25) is obtained, concluding the proof. \blacksquare

The above-designed LQ controller does not ensure that the input constraints (6) are fulfilled. Therefore, in what follows, a positively invariant region associated to the closed-loop dynamics (23) and complying with (6) is derived exploiting the worst-case inner approximation \hat{U} of (6).

Theorem 1: Consider a constant reference signal \bar{z}_r and the closed-loop error model (23) where the gain K is designed as in (25). The set

$$\tilde{\mathcal{Z}} = \{\tilde{z} \in \mathbb{R}^2 \mid \tilde{z}^T S \tilde{z} \leq 1\}, \quad S = \frac{\kappa^2}{\hat{\rho}^2} I_{2 \times 2} \quad (28)$$

is positively invariant and it complies with the input constraint set (6) irrespectively of any $\theta \in \mathbb{R}$ and $\varphi \in (-\pi/2, \pi/2)$.

Proof: First, the set $\tilde{\mathcal{Z}} \subset \mathbb{R}^2$ of initial states $\tilde{z}(0) = z(0) - \bar{z}_r$ such that the LQ controller (22), with the gain K as in (25), does not violate the input constraints $\forall \theta \in \mathbb{R}, \varphi \in (-\pi/2, \pi/2)$ can be found substituting (22) in the worst-case input constraint set (9), obtaining (28). As shown in [17], a generic ellipsoidal set

$$\mathcal{E} = \{\tilde{z} \in \mathbb{R}^2 \mid \tilde{z}^T S \tilde{z} \leq 1\} \quad (29)$$

is positively invariant for (23) if

$$(A - BK)^T S (A - BK) - S < 0 \quad (30)$$

Given that $\tilde{\mathcal{Z}}$ is equal to (29) if $S = K^T \frac{1}{r^2} I_{2 \times 2} K = \frac{\kappa^2}{r^2} I_{2 \times 2}$, the set (28) is positively invariant for (23) if

$$\frac{\kappa^2}{r^2} ((A - BK)^T I (A - BK) - I) < 0 \quad (31)$$

Since A, B, K are scalar matrices, then $A - BK$ is also a scalar matrix containing on the diagonal the closed-loop eigenvalues, i.e., $A - BK = \lambda I_{2 \times 2}$. Moreover, since $w(k) = -K \tilde{z}(k)$ is stabilizing, then $|\lambda| < 1$, $(A - BK)^T I (A - BK) - I < 0$ and the condition (31) is fulfilled. ■

Note that the controller (22) has been designed considering the offset-free model (21). Consequently, the actual tracking error (18a) is not guaranteed to remain in $\tilde{\mathcal{Z}}$ for any reference signal. However, since $\tilde{\mathcal{Z}}$ enjoys contractivity under (22), then $\tilde{\mathcal{Z}}$ is also robustly invariant for (18a) under a sufficient small disturbance $w_r(k)$ [18]. Moreover, under Assumption 1, $w_r(k)$ is bounded and can be over approximated (for a given reference trajectory) as a circular set $\mathcal{W}(r_d)$ of radius $r_d > 0$, where $\mathcal{W}(r_d) = \{w_r \in \mathbb{R}^2 \mid w_r^T W_{r_d} w_r \leq 1\}$, $W_{r_d} = \frac{1}{r_d^2} I_{2 \times 2}$. Consequently, $\tilde{\mathcal{Z}}$ is robustly invariant $\forall w_r(k) \in \mathcal{W}(r_d)$ if $(A - BK) \tilde{\mathcal{Z}} \subseteq \tilde{\mathcal{Z}} \sim B \mathcal{W}(r_d)$ [18], where \sim is the Minkowski set difference operator. Given that all the involved sets have a circular shape, the above set containment condition can be equivalently rewritten as the following matrix inequality (adapted from [18, Section 3]):

$$\eta^{-1} (A - BK)^T S^{-1} (A - BK) + (1 - \eta)^{-1} B^T W_{r_d}^{-1} B \leq S^{-1} \quad (32)$$

where $\eta = 1 - \sqrt{\xi}$ and ξ is the only repeated eigenvalue of the matrix $G^T B^T W_{r_d}^{-1} B G$, with G such that $G^T S^{-1} G = I_{2 \times 2}$.

Theorem 2: If the reference trajectory (17) complies with Assumption 1 and the condition (32) is fulfilled, then $\tilde{\mathcal{Z}}$ is robustly invariant for (20) under (22). Moreover, if $\tilde{z}(0) \in \tilde{\mathcal{Z}}$, the nonlinear state-feedback tracking control law

$$u(k) = -M^{-1}(\theta(k), \varphi(k)) K(z(k) - \hat{z}_r(k)) \quad (33)$$

ensures stable full-state tracking (see Definition 3) and input constraints (2) fulfillment for the car-like vehicle (1).

Proof: First, as proved in Theorem 1, for any initial error in $\tilde{\mathcal{Z}}$ and constant reference, the control law (22), with K as in (25), asymptotically stabilizes (23) while fulfilling (by worst-case) the input constraints (6). On the other hand, if $z_r(k)$ is a generic reference trajectory complying with Assumption 1 such that the corresponding disturbance $-w_r(k)$ in (20a) is bounded by a set $\mathcal{W}(r_d)$ that fulfills the condition

(32), then, the control law (22) ensures that $\tilde{\mathcal{Z}}$ is robustly invariant irrespectively of $w_r(k)$ and that the evolution of (20a) is stable. Consequently, given the results stated in Lemma 1, the nonlinear control law (33) (obtained applying the inverse transformation of (4) to (22)) ensures full-state tracking and constraint (2) fulfillment for the car-like model (1). ■

IV. SIMULATION RESULTS

In this section, the effectiveness of the proposed tracking controller is shown. The simulations have been performed in Matlab, where the car-like model (1) has been configured with the following set of parameters: $l = 0.5m$, $\bar{v} = 0.5m/s$, and $\bar{\omega} = \frac{\pi}{4} RAD/s$. Moreover, we have assumed that the coordinates $x(t)$ and $y(t)$, the orientation $\theta(t)$, and steering angle $\varphi(t)$ of the car are available for control purposes. The car-like model has been feedback linearized using the transformations (3)-(4) and setting $\Delta = 0.35m$. Consequently, by applying the formula in (9), the radius of the worst-case input constraint set (9) for the linearized model (18a) is $\hat{r} = 0.2252$. Then, the linearized car model has been discretized using a sampling time $T_s = 0.1$ sec, and the used LQ parameters are $q = 1$ and $\rho = 0.01$ (see Proposition 3). Consequently, the control gain K computed as in (25) is $K = 6.1803 I_{2 \times 2}$, and the positively invariant region associated to this controller is obtained as in (28) and it is characterized by a shaping matrix $S = 753.1737 I_{2 \times 2}$. The resulting positively invariant region is shown in Fig. 5 by means of a red solid line. In the performed simulation, the reference signal has an eight-shape and its timing law in the $x - y$ plane is (see the dashed red line in Fig. 3)

$$x_r(t) = \sin(t/10), \quad y_r(t) = \sin(t/20)$$

The reference velocities \dot{x}_r, \dot{y}_r and accelerations \ddot{x}_r, \ddot{y}_r have been obtained from the above via differentiation, and the corresponding orientation θ_r and steering angle ϕ_r computed via (17). For the chosen reference and control parameters, we have that $r_d = 0.1838$, $\eta = 0.4956$ and that the condition (32) is fulfilled. Moreover, the car's initial conditions are assumed to be $x_0 = 0, y_0 = -0.035, \theta_0 = 0, \varphi_0 = 0$.

The obtained simulation results are collected in Figs. 3-5. Specifically, In Fig. 3, it is possible to appreciate the tracking capability of the considered controller, even though the initial car's initial point (see the yellow star) is far from the desired trajectory. Fig. 4 shows that the car's linear and steering velocities ($v(t)$ and $\omega(t)$) fulfill the prescribed constraints (see the dashed red line in the first two subplots) regardless of the robot's angles $\theta(t)$ and $\varphi(t)$, confirming the correctness of the used worst-case approximation of the car's constraints. Moreover, the small discrepancies between the angles of the vehicle $\theta(k)$ and $\varphi(k)$ and their reference value $\theta_r(r)$ and $\varphi_r(k)$, testify that the evolution of the tracking error internal dynamics is bounded and actually in the proximity of the reference trajectories. Finally, Fig. 5 shows that the linear system's tracking error trajectory $\tilde{z}(t) = z(t) - \hat{z}_r(t)$ (blue solid line) is confined in $\tilde{\mathcal{Z}}$ (red solid circle), confirming that the joint use of the proposed feasibility governor and constrained tracking controller make $\tilde{\mathcal{Z}}$ positively invariant.

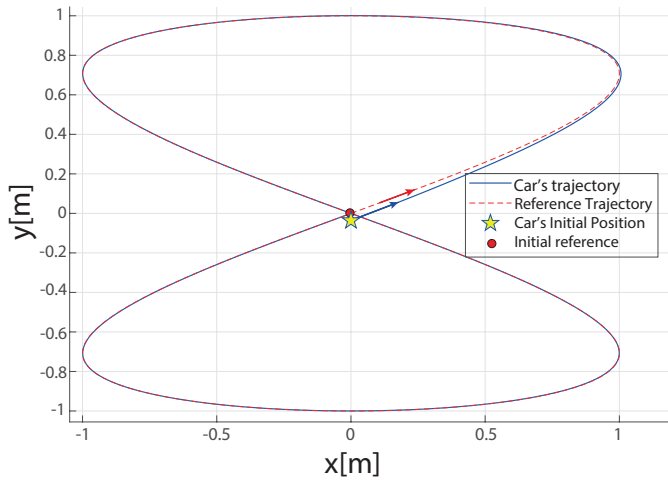


Fig. 3. Trajectory tracking.

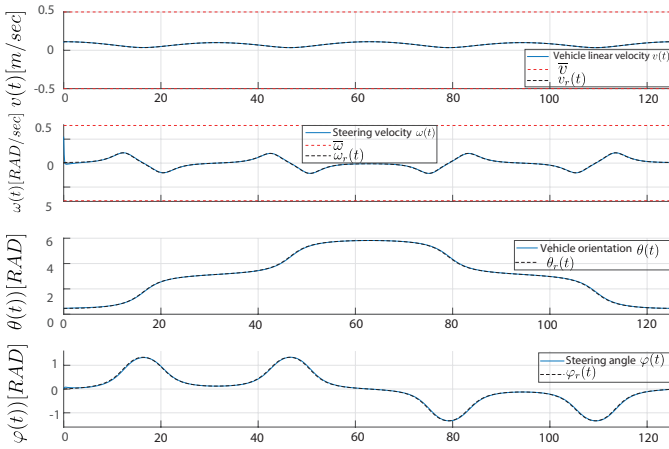


Fig. 4. Car's velocities and angles.

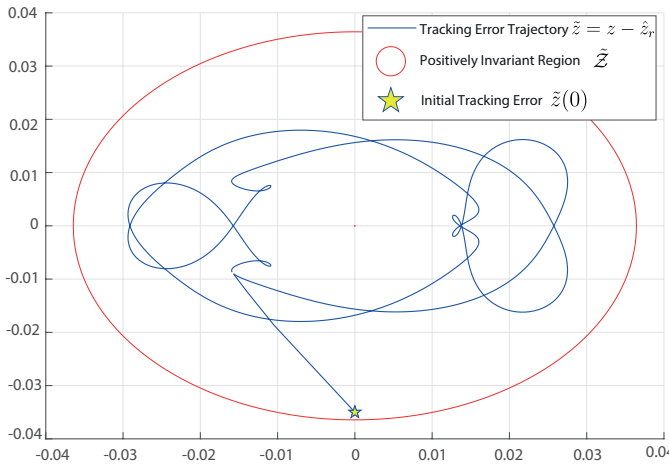


Fig. 5. Trajectory tracking error for the feedback linearized car-like model and positively invariant region $\tilde{\mathcal{Z}}$.

V. CONCLUSIONS

In this paper, we have shown that it is possible to design a constrained tracking controller with associated control invariant region for an input constrained feedback linearized car-like vehicle. This has been obtained by properly deriving a

worst-case approximation of the time-varying input constraints arising when the nonlinear car model is feedback linearized. Such a characterization of the constraint set has been then exploited to design a state-feedback controller where the associated invariant region is analytically derived. Although the proposed solution can be used as a standalone constrained tracking controller, its features might allow using it as the terminal controller of dual-mode predictive controller strategies. Future studies will be devoted to investigating such a possibility.

REFERENCES

- [1] B. Paden, M. Čáp, S. Z. Yong, D. Yershov, and E. Frazzoli, "A survey of motion planning and control techniques for self-driving urban vehicles," *IEEE Trans. on Intelligent Vehicles*, vol. 1, no. 1, pp. 33–55, 2016.
- [2] N. H. Amer, H. Zamzuri, K. Hudha, and Z. A. Kadir, "Modelling and control strategies in path tracking control for autonomous ground vehicles: a review of state of the art and challenges," *Journal of Intelligent & Robotic Systems*, vol. 86, no. 2, pp. 225–254, 2017.
- [3] A. De Luca, G. Oriolo, and C. Samson, "Feedback control of a nonholonomic car-like robot," *Robot Motion Planning and Control*, pp. 171–253, 1998.
- [4] M. Rokonuzzaman, N. Mohajer, S. Nahavandi, and S. Mohamed, "Review and performance evaluation of path tracking controllers of autonomous vehicles," *IET Int. Transport Systems*, vol. 15, no. 5, pp. 646–670, 2021.
- [5] F. Eiras, M. Hawasly, S. V. Albrecht, and S. Ramamoorthy, "A two-stage optimization-based motion planner for safe urban driving," *IEEE Trans. on Robotics*, vol. 38, no. 2, pp. 822–834, 2021.
- [6] K. Majd, M. Razeghi-Jahromi, and A. Homaifar, "A stable analytical solution method for car-like robot trajectory tracking and optimization," *IEEE/CAA Journal of Automatica Sinica*, vol. 7, no. 1, pp. 39–47, 2019.
- [7] J. Deng, V. Becerra, and R. Stobart, "Input constraints handling in an MPC/feedback linearization scheme," *Int. Journal of Applied Mathematics and Computer Science*, vol. 19, no. 2, pp. 219–232, 2009.
- [8] D. Angeli, A. Casavola, G. Franzè, and E. Mosca, "An ellipsoidal off-line MPC scheme for uncertain polytopic discrete-time systems," *Automatica*, vol. 44, no. 12, pp. 3113–3119, 2008.
- [9] E. F. Camacho and C. Bordons, "Nonlinear model predictive control," in *Model Predictive Control*. Springer, 2007, pp. 249–288.
- [10] F. Blanchini, "Set invariance in control," *Automatica*, vol. 35, no. 11, pp. 1747–1767, 1999.
- [11] R. Kianfar, P. Falcone, and J. Fredriksson, "Safety verification of automated driving systems," *IEEE Int. Transportation Systems Magazine*, vol. 5, no. 4, pp. 73–86, 2013.
- [12] P. Falcone, M. Ali, and J. Sjöberg, "Predictive threat assessment via reachability analysis and set invariance theory," *IEEE Trans. on Intelligent Transportation Systems*, vol. 12, no. 4, pp. 1352–1361, 2011.
- [13] K. Berntorp, A. Weiss, C. Danielson, I. V. Kolmanovsky, and S. Di Cairano, "Automated driving: Safe motion planning using positively invariant sets," in *Int. Conference on Int. Transportation Systems (ITSC)*. IEEE, 2017, pp. 1–6.
- [14] F. Borrelli, A. Bemporad, and M. Morari, *Predictive Control for Linear and Hybrid Systems*. Cambridge University Press, 2017.
- [15] D. Wang and G. Xu, "Full-state tracking and internal dynamics of nonholonomic wheeled mobile robots," *IEEE/ASME Trans. on Mechatronics*, vol. 8, no. 2, pp. 203–214, 2003.
- [16] B. D. Anderson and J. B. Moore, *Optimal Control: Linear Quadratic Methods*. Courier Corporation, 2007.
- [17] F. Blanchini and S. Miani, *Set-theoretic Methods in Control*. Springer, 2008, vol. 78.
- [18] I. Kolmanovsky and E. G. Gilbert, "Theory and computation of disturbance invariant sets for discrete-time linear systems," *Mathematical problems in engineering*, vol. 4, no. 4, pp. 317–367, 1998.